CHAPTER 147

WAVE LOADS ON HORIZONTAL CYLINDERS

by

P. Holmes[1] and J. R. Chaplin[2]

INTRODUCTION

The problem of predicting wave induced loads on cylinders is an enormously complex one. It is clear from the scatter present in most experimental determinations of force coefficients that there are many individual factors which influence the mechanisms of flow induced loading. Among these are some, for instance Reynolds number, separation and periodic vortex shedding, which are inter-related and whose influences cannot be studied in isolation. Others, such as shear flow, irregular waves and free surface effects, can at least be eliminated in the laboratory, in order to approach an understanding of the more fundamental characteristics of the flow.

A vertical cylinder in uniform waves experiences an incident flow field which can be described in terms of rotating velocity and acceleration vectors, always in the same vertical plane, containing also the cylinder axis, whose magnitudes are functions of time and of position along the length of the cylinder. Some of the essential features of this flow can be studied under two-dimensional oscillatory conditions, in which either the cylinder or the fluid is oscillated relative to the other along a straight line (planar oscillatory flow). The incident velocity and acceleration vectors are then always concurrent, normal to the cylinder axis, and oscillating in magnitude with time.

According to Morison's equation (1), the total force per unit length on the cylinder in line with the velocity and acceleration vectors in this context, is the sum of the drag and inertia components:

$$F = F_d + F_i = C_d \frac{1}{2} \rho \, d \, U|U| + C_m \frac{\pi d^2}{4} \rho \frac{dU}{dt} \qquad (1)$$

where C_d and C_m are the time-independent drag and inertia coefficients, U the instantaneous flow velocity, ρ the fluid density and d the cylinder diameter. From experiments in planar oscillatory flow around smooth cylinders, Sarpkaya (2, 3) found that C_d and C_m are functions of the Keulegan Carpenter number, $K_c = U_{max} T/d$, where T is the period of oscillation, and of the Reynolds number, $R_e = U_{max} d/\upsilon$, when it is

---

1. Professor of Maritime Civil Engineering, University of Liverpool, U.K.

2. Lecturer in Civil Engineering, University of Liverpool, U.K.

greater than about 2×10^4. Sarpkaya derived C_d and C_m from force records by a Fourier-averaging procedure.

Very much less attention has been given to wave loads on horizontal cylinders, although many characteristics of the flow are qualitatively different from those relating to vertical cylinders. Most of the investigations on horizontal cylinders have concentrated on the effects proximity of the ocean bottom (4, 5, 6), so that particle orbits in the region of the cylinder were fairly flat ellipses. In some cases the flow is assumed to be planar oscillatory as described above. Maull and Norman (7) measured wave forces on horizontal cylinders where particle orbits were almost circular and analysed the results in terms of horizontal and vertical load components. It is more instructive, however, to study the load components which are in line with the velocity and acceleration vectors respectively, since the drag and inertial contributions are then more readily distinguished. In the particular case when particle orbits in the region of the cylinder are circular, the incident flow around the cylinder is represented approximately by uniform flow described by a rotating velocity vector of constant magnitude. The actual flow deviates from this uniform condition as a result of the phase differences in the direction of wave propagation between particle motion on adjacent orbits, and because of the exponential decay of particle velocities with depth. However, providing the diameter of the cylinder is small compared with the wavelength the assumption of uniform ambient flow is a reasonable one. The undisturbed flow conditions around the cylinder can then be specified very simply. As in the case of the idealisation of flow around vertical cylinders in waves by planar oscillatory flow, some of the essential features of horizontal cylinders in waves can be represented in isolation. The ambient flow consists of a body of water moving without distortion or rotation around a circular orbit at the centre of which is the axis of the cylinder. The incident velocity and acceleration vectors are now of constant magnitude, rotating with constant angular velocity once in every wave period, with the latter leading the former by 90°. In this context the components of Morison's equation for force per unit length may be written:

$$F_d = \rho C_d \frac{1}{2} \rho d \Omega^2 R^2 \qquad (2)$$

and

$$F_i = C_m \frac{\pi d^2}{4} \rho \Omega^2 R \qquad (3)$$

where F_d and F_i are respectively drag and inertia load per unit length, Ω is the wave angular frequency and R the radius of the particle orbit. The components F_d and F_i act in the directions of the velocity and acceleration vectors respectively and are thus now orthogonal. It is worth noting that viewed from a frame of reference centred on the axis of the cylinder and rotating with the wave frequency, the ambient flow, but for the re-cycling of the previously generated wake, is steady. Moreover, fluctuations with time in F_d and F_i can be caused only by this disturbed incident flow resulting from the previously generated wake, and by vortex shedding.

Like planar oscillatory flow, this simplified model of circular irrotational ambient flow around a cylinder can be used in the laboratory to reproduce some features of wave loading, in the absence of others which normally add to the complexity of interpreting experimental data. It is perhaps closer to the widely studied case of steady uni-directional flow around cylinders since the interference of the wake on the incident flow is less pronounced, and the magnitude of the velocity is steady. The analytical methods used to investigate separated flow around cylinders, such as the finite difference solution for the time-dependent Navier-Stokes equations (8), or the discrete vortex model (9), may be used also in this context without fundamental changes. However, they remain restricted or incomplete, and require experimental data for verification.

The purpose of this paper is to describe an experiment in which circular irrotational ambient flow around a cylinder was modelled by moving a cylinder without rotation around a circular orbit in initially still water. Allowing for the changed frame of reference, the motion of the fluid is identical in the two cases. However, forces experienced by the cylinder differ due to the presence of a pressure gradient in the fluid on the one hand and to the inertia of the cylinder itself on the other. The difference may easily be calculated, as shown below. Forces experienced by the cylinder were monitored continuously with time for Reynolds numbers in the range 0.4×10^5 to 2.4×10^5 and for Keulegan Carpenter numbers of 12.8, 24.0 and 35.7.

APPARATUS

The tests were carried out in a tank about 5m. square in plan, in a water depth of 90cm. The cylinder was supported with its axis vertical from an arm which rotated above the water surface about a central pivot. The apparatus is shown in Fig. 1. A one horsepower variable speed motor provided the drive to the central shaft and was mounted on the side of the tank to minimise vibrations in the cylinder support. In order that the cylinder should pass around its orbit without rotation, a secondary drive belt was provided between its axial support and a fixed central pulley. A number of alternative interchangeable belts facilitated different orbital radii. The use of toothed rubber timing belts throughout ensured perfectly synchronous rotation between the motor, the central drive shaft and the cylinder itself. A simple potentiometer with its end stops removed was connected to the motor and acted as an angular displacement transducer, from the output of which also the angular velocity of the arm could be derived.

The cylinder was mounted axially on a 5cm. diameter hollow alloy tube, cantilevered vertically downwards from the rotating arm, instrumented near its upper end with orthogonal pairs of strain gauges. Since the cylinder and its support did not undergo rotation the cable to the gauges was not subject to any overall twisting and could be connected directly to the conditioning instruments. The cylinder was made out of 15cm. diameter perspex tube of 10mm. wall thickness, and was airtight to minimise its mass. Its natural frequencies in air and water were respectively 14 Hz. and 9 Hz. End discs of diameter 25cm. were mounted on the cylinder as shown in Fig. 1. At its upper end a larger disc of diameter 60cm. was mounted on the fixed cylinder to minimise free surface interference on the instrumented cylinder.

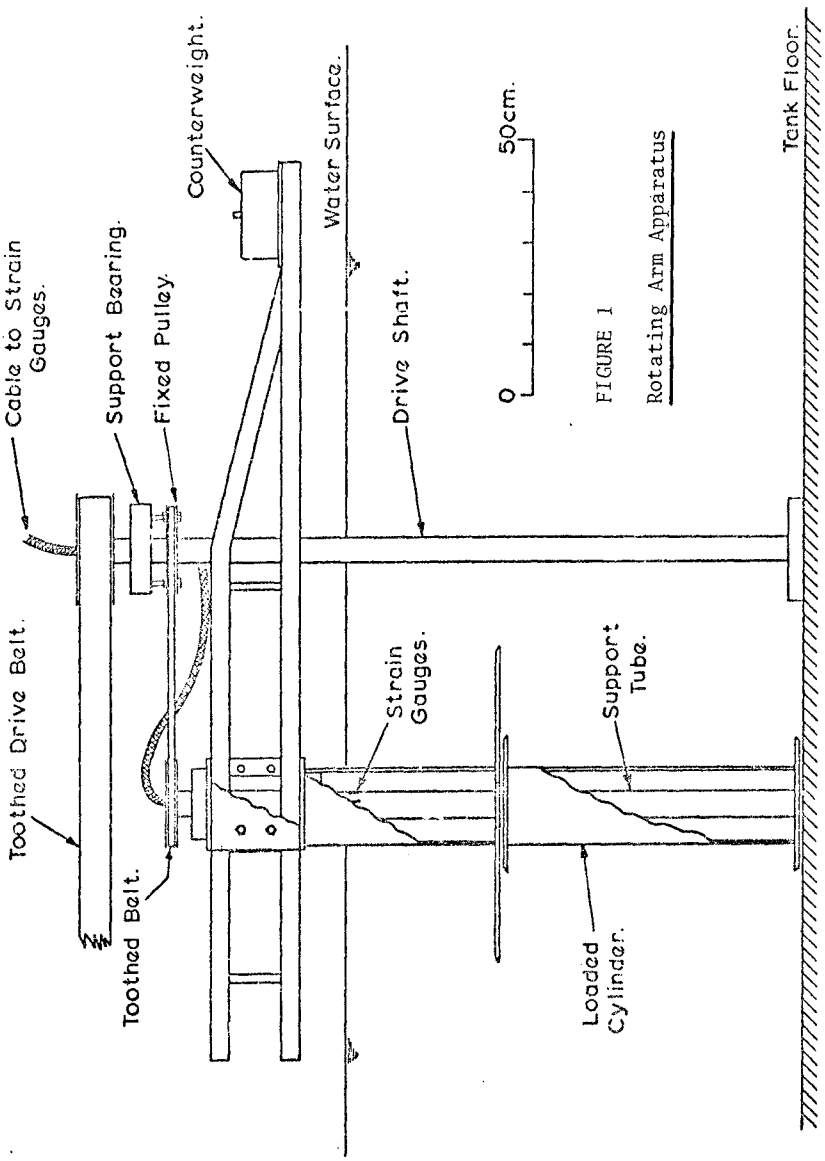

FIGURE 1

Rotating Arm Apparatus

Experiments were run on-line to a Data General Nova Computer which sampled the unfiltered outputs of the strain gauge amplifiers and angular displacement transducer at a frequency of 100 Hz. With the available core, maximum run time was about 40 seconds. The data was processed immediately after each test to provide radial and tangential load components (since the orientation of the gauges rotated with respect to the radial direction during each rotation) and velocities. Besides further digital processing the data was then available for conversion back to analogue form for plotting at a reduced speed on a pen recorder.

Initial strain gauge calibrations were carried out by loading the cylinder at its centre from weights hung over a pulley at the side of the tank. From subsequent tests in air, the effective mass of the cylinder and its support was determined from the outputs of the gauges responding to centrifugal forces. A more rapid method of calibration was then possible, since during each revolution of the apparatus in air, the strains in the cylinder support tube oscillated about zero. A sinusoid was fitted by least squares to the output of each pair of gauges from which their sensitivities and absolute orientations were derived. This method of calibration was applied before and after each series of tests, and in every case the stability of the gauges and instruments was found to be satisfactory. The effective mass of the cylinder and support was 5.47 kg.

RESULTS AND DISCUSSION

According to Morison's equation, the forces per unit length experienced by a cylinder passing around a circular orbit in otherwise still water are:

$$F_d = C_d \frac{1}{2} \rho \, d \, \Omega^2 \, R^2 \tag{4}$$

and

$$F_i = C_a \frac{\pi d^2}{4} \rho \, \Omega^2 \, R + M \, \Omega^2 \, R \tag{5}$$

where R is the orbit radius, M the mass per unit length of the cylinder. The added mass coefficient C_a is given by $C_a = C_m - 1$. The primary object of the experiments described here was to investigate C_d and C_a as functions of the Reynolds number R_e and the Keulegan Carpenter number K_c. The components F_d and F_i correspond to the mean tangential and radially outward forces respectively measured on the cylinder. The derived values for C_d and C_a are time averaged; it is worth noting that since F_d and F_i are orthogonal, C_d and C_a can be derived independently.

In an ideal fluid $C_a = 1$. Although this result is normally derived in the context of concurrent velocity and acceleration vectors, it applies to all cases, whatever their relative orientations.

Tests were carried out with the 15cm. diameter cylinder located at three different radii on the rotating arm: 0.306m, 0.572m. and 0.852m. Since the Keulegan Carpenter number is given by:

$$K_c = \frac{2\pi R}{d} \tag{6}$$

its value is independent of the speed of rotation, by which the Reynolds number is determined:

$$R_e = \frac{\Omega R d}{\upsilon} \tag{7}$$

The three radii used in the tests correspond to K_c values of 12.8, 24.0 and 35.7, respectively. The appearance of K_c and R_e directly as the independent parameters of the experiment is an advantage, since the flow-induced loads are expected to be functions of them only for rigid smooth cylinders.

Fig. 2 presents typical records of tangential and radial loads derived from the strain gauge outputs. In both cases the cylinder was accelerated from rest at the beginning of the record to a constant angular velocity. The first revolution of the cylinder around its orbit is characterised by abnormally high drag and oscillating lift associated with strong vortex shedding. Subsequently the cylinder passes into its own wake and the disturbances present result in a reduction in drag and oscillating lift. After two or three revolutions the mean drag and inertial loads stabilise and show very little variation with time. It is worth noting that the motion of the cylinder resulted in little overall rotation of the water in the tank, which would have caused a progressive reduction in flow-induced forces owing to reducing relative incident velocities. It is reasonable to assume that the cylinder does not stir the tank appreciably for the following reasons. Firstly, its dimensions are small compared with those of the tank itself. Secondly, the cylinder does not rotate; disregarding preferential decay of vorticity of one sense of rotation there is therefore no net addition of vorticity to the water in the tank from the motion of the cylinder.

Radial force records show fluctuations of irregular magnitudes at a frequency corresponding to a Strouhal number of about 0.2. Drag and added mass coefficients are presented in Fig. 3 as functions of R_e and K_c. Each point is derived from the mean radial and tangential force components recorded over a period of about 40 seconds. In each case three or four revolutions were completed before the recording was begun. Fig. 3 clearly shows that with increasing R_e, there is a reduction in C_d and an increase in C_a, depending also on K_c. Although it is clear that the reduction in C_d follows the expected behaviour close to transitional R_e, it is not easy to account for the equally dramatic change in C_a. In contrast to uniform or planar oscillatory flow around a cylinder, in the present case the orbital motion must result in asymmetry of the time-averaged characteristics of the wake. Although the rates at which vorticity is shed in the two shear layers are equal, the outer shear layer must be weaker since its separation point is moving away through the fluid more rapidly than that of the inner shear layer. This causes the vortex shedding to be an asymmetrical process, with unequal proportions of the shed vorticity finding its way into the major

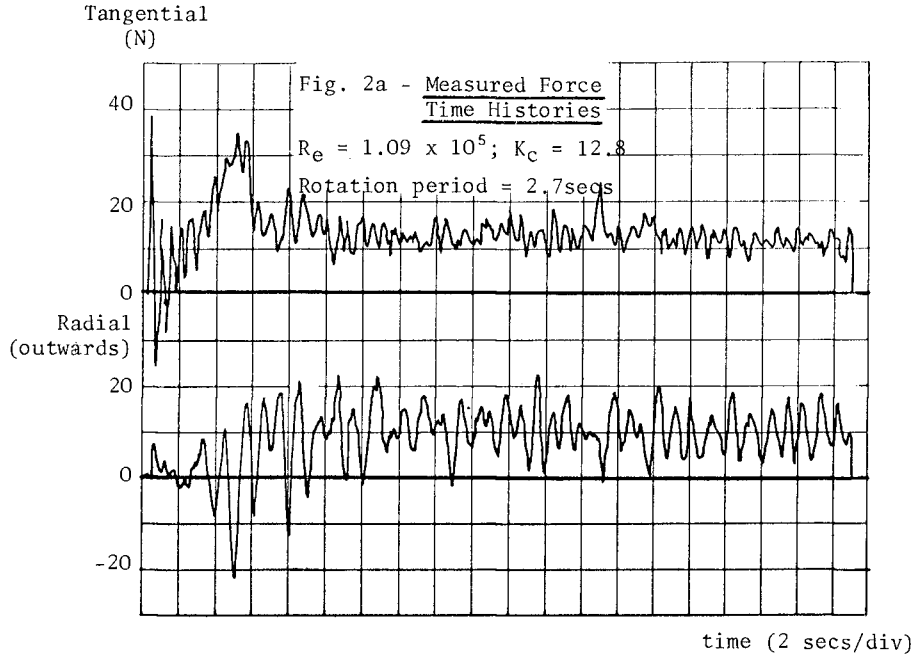

Fig. 2a - Measured Force Time Histories

R_e = 1.09 x 10^5; K_c = 12.8

Rotation period = 2.7secs

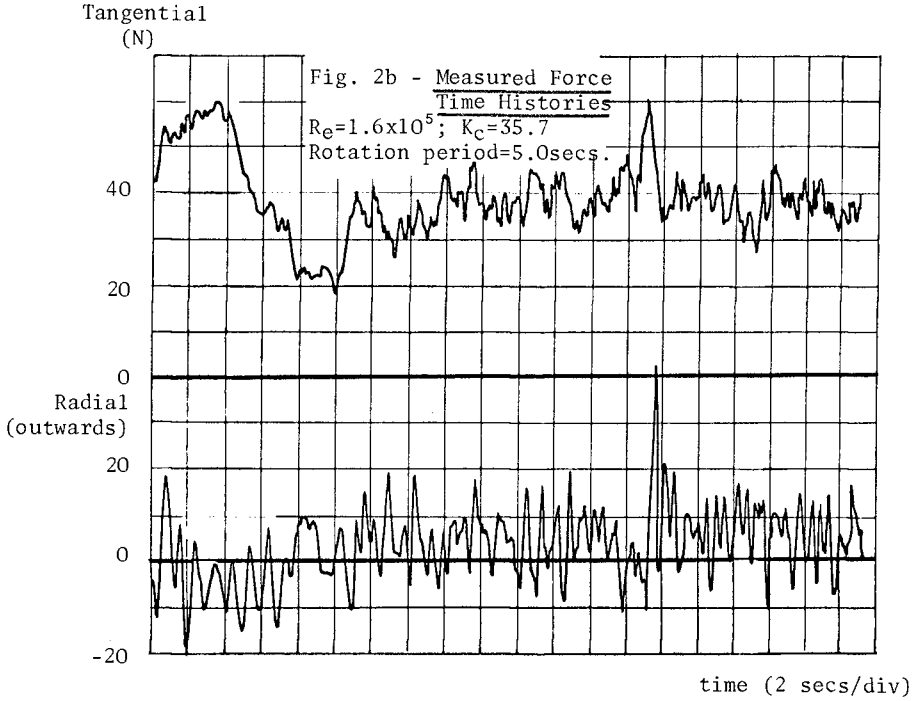

Fig. 2b - Measured Force Time Histories

R_e=1.6x10^5; K_c=35.7

Rotation period=5.0secs.

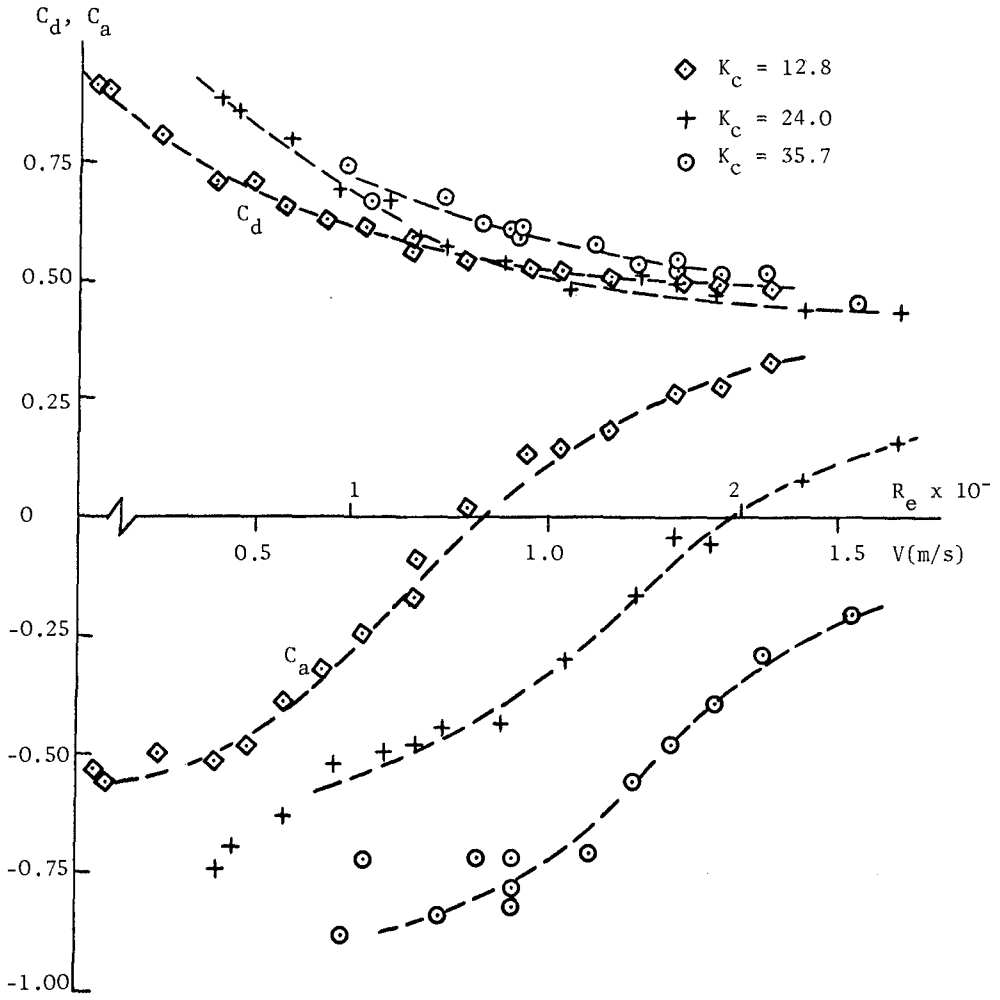

FIGURE 3

Drag Coefficient and Added Mass Coefficient as Functions of Reynolds Number a
Keulegan Carpenter Numbers

vortices of alternate senses of rotation. Possibly modification of this mechanism at transitional Reynolds numbers causes the observed changes in C_a.

However, despite the obvious differences in flow conditions, it is interesting to compare the present results with those obtained by Sarpkaya (3) for planar oscillatory flow around a cylinder. Lines fitted to the data have been re-plotted with Sarpkaya's results in Figs. 4 and 5, where it is shown that there exists at least some qualitative agreement between the two sets of data. Agreement between inertia coefficients would suggest that the added mass of the cylinders were independent of the relative orientations of the velocity and acceleration vectors. As mentioned previously, this would be the case in an ideal fluid, but in a real fluid it is reasonable to expect that the effects of viscosity and the history of the flow would make contributions to the added mass. Qualitative agreement between the two sets of data would also suggest that a conceptual explanation of the observed changes at transitional Reynolds numbers must be sought in terms of the features common to both cases.

CONCLUSIONS

Circular orbital flow around a cylinder has been modelled experimentally by moving a cylinder around a circular path in otherwise still water. The nature of the resulting flow warrants further investigation since it displays many of the essential features present in wave-induced flow around cylinders, and yet is specified very simply.

With increasing Reynolds number over the range 0.4×10^5 to 2.4×10^5 the drag coefficient was found to fall from about 0.9 to 0.4, depending also on Keulegan Carpenter number. Simultaneously the added mass coefficient increased, becoming positive only for higher Reynolds numbers. In both respects the present results are in qualitative agreement with those of Sarpkaya (3) for planar oscillatory flow.

REFERENCES

1. Morison, J. R., O'Brien, M. P., Johnson, J. W. and Schaaf, S. A. 'The force exerted by surface waves on piles', Petroleum transactions, AIME, Vol. 189, 1950, p.149.

2. Sarpkaya, T. 'Forces on cylinders and spheres in a sinusoidally oscillating fluid', Journal of Applied Mechanics, ASME, March 1975, p.32.

3. Sarpkaya, T. 'Vortex shedding and resistance in harmonic flow about smooth and rough circular cylinders', Proc of First Int. Conf. on Behaviour of Offshore Structures, Trondheim, 1976, p.220.

4. Yamamoto, T. and Nath, J. H. 'High Reynolds number oscillating flow by cylinders', Proc. of 15th Int. Conf. on Coastal Engineering, Hawaii, 1976, p.2321.

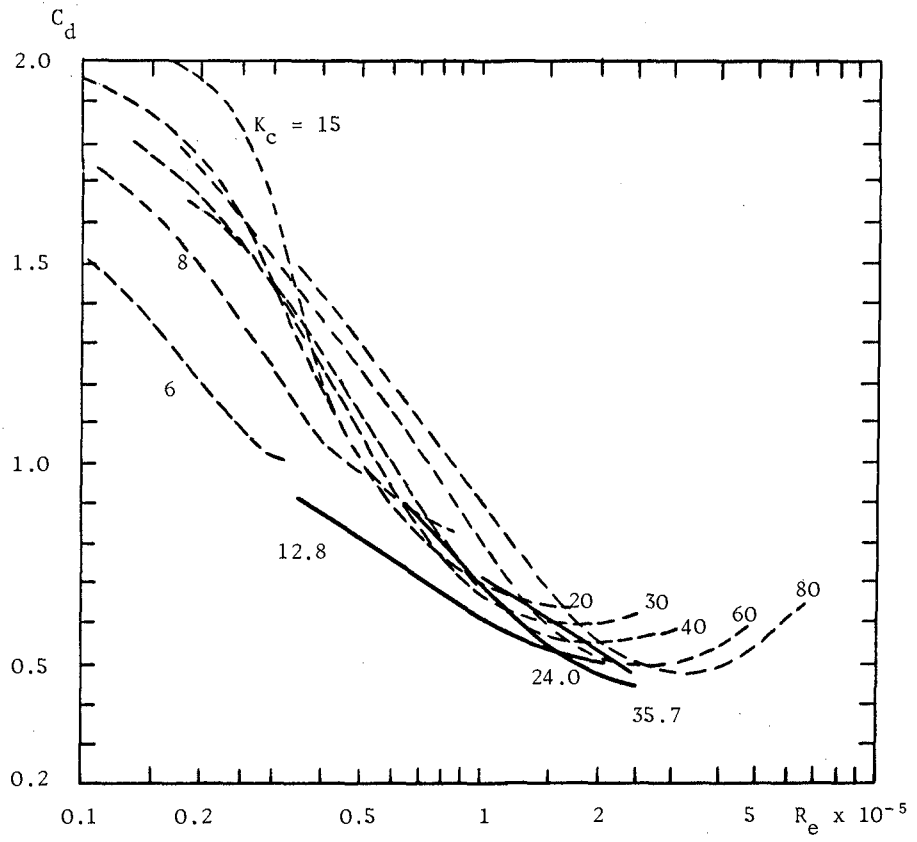

FIGURE 4

Drag Coefficient as A Function of Reynolds Number and Keulegan Carpenter Number

Dashed lines - Sarpkaya (Ref. 3); Solid lines - present results

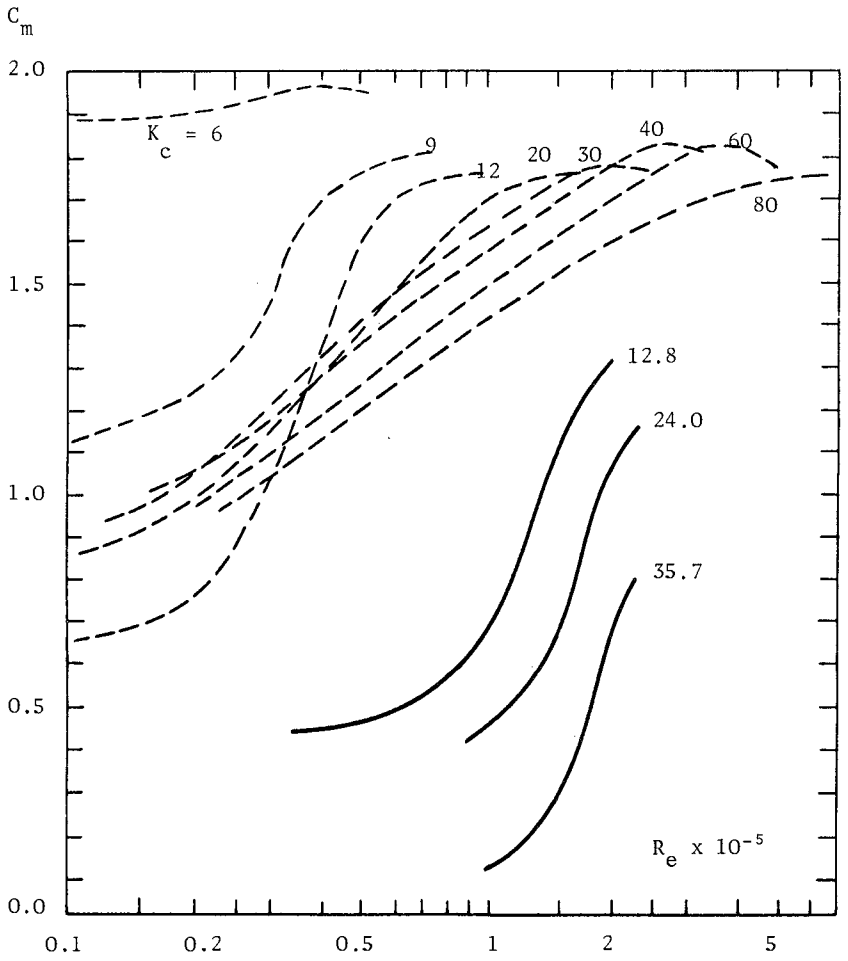

FIGURE 5

Inertia Coefficient as a Function of Reynolds Number and Keulegan Carpenter Number

Dashed Lines - Sarpkaya (Ref. 3); Solid lines - present results.

5. Nath, J. H., Yamamoto, T. and Wright, J. C. 'Wave forces on pipes near the ocean bottom', Proc. of Offshore Technology Conference, Houston, May 1976, OTC 2496.

6. Sarpkaya, T. 'Forces on cylinders near a plane boundary in a sinusoidally oscillating fluid', Fluid Mechanics in the Petroleum Industry, ASME, Dec. 1975, p.43.

7. Maull, D. J. and Norman, S. G. 'A horizontal cylinder in waves', Proc. of Symposium on Mechanics of Wave-Induced Forces on Cylinders, Sept. 1978, Bristol, U.K.

8. Roache, P. J. 'Computational Fluid Dynamics', Hermosa, Albequerque, 1972.

9. Stansby, P. K. 'An inviscid model of vortex shedding from a circular cylinder in steady and oscillatory far flows', Proc. Inst. Civ. Engrs. Vol. 63, Part 2, 1977, p.865.